

Constraints on First-Light Ionizing Sources from Optical Depth of the Cosmic Microwave Background

J. Michael Shull & Aparna Venkatesan¹

*University of Colorado, Department of Astrophysical & Planetary Sciences,
CASA, 389-UCB, Boulder, CO 80309*

michael.shull@colorado.edu, avenkatesan@usfca.edu

ABSTRACT

We examine the constraints on high-redshift star formation, ultraviolet and X-ray pre-ionization, and the epoch of reionization at redshift z_r , inferred from the recent WMAP-5 measurement, $\tau_e = 0.084 \pm 0.016$, of the electron-scattering optical depth of the cosmic microwave background (CMB). Half of this scattering can be accounted for by the optical depth, $\tau_e = 0.04\text{--}0.05$, of a fully ionized intergalactic medium (IGM) at $z \leq z_{\text{GP}} \approx 6\text{--}7$, consistent with Gunn-Peterson absorption in neutral hydrogen. The required additional optical depth, $\Delta\tau_e = 0.03 \pm 0.02$ at $z > z_{\text{GP}}$, constrains the ionizing contributions of “first light” sources. WMAP-5 also measured a significant increase in small-scale power, which lowers the required efficiency of star formation and ionization from mini-halos. Early massive stars (UV radiation) and black holes (X-rays) can produce a partially ionized IGM, adding to the residual electrons left from incomplete recombination. Inaccuracies in computing the ionization history, $x_e(z)$, and degeneracies in cosmological parameters (Ω_m , Ω_b , σ_8 , n_s) add systematic uncertainty to the measurement and modeling of τ_e . From the additional optical depth from sources at $z > z_{\text{GP}}$, we limit the star-formation efficiency, the rate of ionizing photon production for Pop III and Pop II stars, and the photon escape fraction, using standard histories of baryon collapse, minihalo star formation, and black-hole X-ray preionization.

Subject headings: cosmology: theory — cosmic microwave background — early universe — intergalactic medium

¹Now at Department of Physics, 2130 Fulton St., University of San Francisco, San Francisco, CA 94117

1. INTRODUCTION

In recent years, an enormous amount of exciting cosmological data have appeared, accompanied by theoretical inferences about early galaxy formation and the first massive stars. Many of these inferences were reactions to first-year (WMAP-1) results (Kogut et al. 2003; Spergel et al. 2003) from the *Wilkinson Microwave Anisotropy Probe* (WMAP). WMAP-1 inferred a high optical depth to the cosmic microwave background (CMB) and suggested early reionization of the intergalactic medium (IGM). Other conclusions came from simplified models for the stellar initial mass function (IMF), atomic/molecular physics, radiative processes, and prescriptions for star formation rates and escape of photoionizing radiation from protogalaxies.

The CMB optical depth and other cosmological parameters have been refined significantly in the recent WMAP-5 data (Hinshaw et al. 2008). In this paper, we use these new measurements to constrain the efficiency of first-light ionizing sources. We focus on the reionization epoch, defined as the redshift z_r when the IGM becomes nearly fully ionized over most of its volume (Gnedin 2000, 2004). Our knowledge about reionization comes primarily from three types of observations: hydrogen Ly α absorption in the IGM, high- z Ly α -emitting galaxies, and CMB optical depth. Optical spectroscopic studies of the “Gunn-Peterson” (Ly α) absorption toward high-redshift quasars and galaxies imply that H I reionization occurred not far beyond $z_{\text{GP}} \sim 6$ (Becker et al. 2001; Fan et al. 2002, 2006). Ultraviolet spectra suggest that He II reionization occurred at $z \sim 3$ (Kriss et al. 2001; Shull et al. 2004; Zheng et al. 2004). The detection of high-redshift (Ly α -emitting) galaxies (Hu & Cowie 2006) suggests a somewhat higher redshift, $z_r \geq 6.5$. Data from WMAP, after three years (Spergel et al. 2007) and five years (Hinshaw et al. 2008), suggest that reionization might occur at $z \approx 10$, with sizeable uncertainties in measuring and modeling the CMB optical depth.

There appears to be a discrepancy between the two epochs, $z_{\text{GP}} \approx 6$ –7 and $z_r \approx 10$. However, the WMAP and Ly α absorption results are not necessarily inconsistent, since they probe small amounts of ionized and neutral gas, respectively. Both the H I absorbers and ionized filaments in the “cosmic web” (Cen & Ostriker 1999) are highly structured at redshifts $z < 10$ and affect the optical depths in Ly α . In order to effectively absorb all the Ly α radiation at $z \approx 6$ requires a volume-averaged neutral fraction of just $x_{\text{HI}} \approx 4 \times 10^{-4}$ (Fan et al. 2006). Simulations of the reionization process (Gnedin 2004; Gnedin & Fan 2006) show that the transition from neutral to ionized is extended in time between $z = 5 - 10$. The first stage (pre-overlap) involves the development and expansion of the first isolated ionizing sources. The second stage marks the overlap of the ionization fronts and the disappearance of the last vestiges of low-density neutral gas. Finally, in the post-overlap stage, the remaining high-density gas is photoionized. The final drop in neutral fraction and increase in photon mean free path occur quite rapidly, over $\Delta z \approx 0.3$.

Initial interpretations of the high WMAP-1 optical depth ($\tau_e = 0.17 \pm 0.03$) were based on models of “sudden reionization”, neglecting scattering from a partially ionized IGM at $z > z_r$. The three-year (WMAP-3) and five-year (WMAP-5) data resulted in considerable downward revisions, with recent measurements giving $\tau_e = 0.084 \pm 0.016$ (Hinshaw et al. 2008; Komatsu et al. 2008). These analyses assumed a single step to complete ionization ($x_e = 1$ at $z \leq z_r$), while Dunkley et al. (2008) also explored a two-step ionization history with a broader distribution of τ_e . The WMAP-5 data alone gave a 5σ detection, $\tau_e = 0.087 \pm 0.017$ (Dunkley et al. 2008), while WMAP-5 combined with distance measurements from Type Ia supernovae (SNe) and baryon acoustic oscillations (BAO) gave $\tau_e = 0.084 \pm 0.016$ (Hinshaw et al. 2008; Komatsu et al. 2008). The single-step analyses gave a reionization epoch $z_r = 10.8 \pm 1.4$ at 68% confidence level (C.L.). The χ^2 curves for two-step ionization provide little constraint on the redshift of reionization or on an IGM with low partial ionization fractions, $x_e \ll 0.1$, as we discuss in § 3. Figure 3 of Spergel et al. (2007) and Figure 8 of Dunkley et al. (2008) show that the parameters x_e and z_r are somewhat degenerate, each with a long tail in the likelihood curves. This emphasizes the importance of contributions to τ_e from ionizing UV photons at $z > z_{\text{GP}}$ from early massive stars and X-rays from accreting black holes (Venkatesan, Giroux, & Shull 2001, hereafter VGS01; Ricotti & Ostriker 2004; Begelman, Volonteri, & Rees 2006).

Models of the extended recombination epoch (Seager, Sasselov, & Scott 2000) predict a partially ionized medium at high redshifts, owing to residual electrons left from incomplete recombination. Residual electrons produce additional scattering, $\Delta\tau_e \approx 0.06$ between redshifts $z \approx 10$ –700. These effects are computed in CMB radiation transfer codes such as CMBFAST and RECFAST, but only a portion of this scattering affects the large angular scales ($\ell \leq 10$) where WMAP detects a polarization signal. X-ray preionization can also produce CMB optical depths $\tau_e \geq 0.01$ (VGS01; Ricotti, Ostriker, & Gnedin 2005).

As we discuss in § 2.1, a fully ionized IGM from $z = 0$ back to $z_{\text{GP}} = 6.1 \pm 0.15$, the reionization epoch inferred from Gunn-Peterson absorption (Gnedin & Fan 2006), produces optical depth, $\tau_e \approx 0.041 \pm 0.003$. This represents nearly half of the WMAP-5 measurement, $\tau_e = 0.084 \pm 0.016$. If the epoch of Gunn-Peterson reionization is $z_{\text{GP}} = 7$ (Wyithe et al. 2008), the contribution is $\tau_e = 0.050 \pm 0.003$. Therefore, the high-redshift ionizing sources are limited to producing an additional optical depth, $\Delta\tau_e \leq 0.03 \pm 0.02$. In § 3, we discuss the resulting constraints on the amount of star formation and X-ray activity at $z \gtrsim 7$. We also parameterize the efficiency of various star formation environments, as determined by halo mass and the metallicity of stellar populations, to address several questions. Can reionization occur at relatively low efficiency, corresponding to star formation in massive Ly α -cooled halos (virial temperature $T_{\text{vir}} \approx 10^4$ K), or must it take place in H₂-cooled minihalos ($T_{\text{vir}} \approx 10^3$ K)? Does one require the high ionizing efficiencies of Population III (metal-free) stars, or can reionization be achieved by lower-efficiency Population II stars?

The IGM is thought to have a complex reionization history, with periods of extended reionization for H I and He II (Venkatesan, Tumlinson, & Shull 2003; Cen 2003; Wyithe & Loeb 2003; Hui & Haiman 2003; Benson et al. 2006). Because τ_e measures the integrated column density of electrons, there are many possible scenarios consistent with the WMAP-5 data. In addition, reionization models are quite sensitive to the amount of “small-scale power” for ionizing sources, which depend on σ_8 , the normalized amplitude of fluctuations.

2. OPTICAL DEPTH TO ELECTRON SCATTERING

2.1. Analytic Calculation of Optical Depth

To elucidate the dependence of CMB optical depth on the epoch of reionization (redshift z_r), we integrate the electron scattering optical depth, $\tau_e(z_r)$, for a homogeneous, fully ionized medium out to z_r . For instantaneous, complete ionization at redshift z_r , we calculate τ_e as the integral of $n_e \sigma_T d\ell$, the electron density times the Thomson cross section along proper length,

$$\tau_e(z_r) = \int_0^{z_r} n_e \sigma_T (1+z)^{-1} [c/H(z)] dz. \quad (1)$$

We adopt a standard Λ CDM cosmology, in which $(d\ell/dz) = c(dt/dz) = (1+z)^{-1}[c/H(z)]$, where $H(z) = H_0[\Omega_m(1+z)^3 + \Omega_\Lambda]^{1/2}$ and $\Omega_m + \Omega_\Lambda = 1$ (no curvature). The densities of hydrogen, helium, and electrons are written $n_H = [(1-Y)\Omega_b \rho_{\text{cr}}/m_H](1+z)^3$, $n_{\text{He}} = y n_H$, and $n_e = n_H(1+y)$, if helium is singly ionized. We assume a primordial helium mass fraction, $Y = 0.2477 \pm 0.0029$ (Peimbert et al. 2007) and define $y = (Y/4)/(1-Y) \approx 0.0823$ as the He fraction by number. Helium contributes 8% to τ_e , assuming single ionization (He II) at $z > 3$. An additional $\tau_e \approx 0.002$ comes from helium reionization to He III at $z \leq 3$ (Shull et al. 2004). The critical density is $\rho_{\text{cr}} = (1.8785 \times 10^{-29} \text{ g cm}^{-3})h^2$ where $h = (H_0/100 \text{ km s}^{-1} \text{ Mpc}^{-1})$. The above integral can be done analytically:

$$\begin{aligned} \tau_e(z_r) &= \left(\frac{c}{H_0}\right) \left(\frac{2\Omega_b}{3\Omega_m}\right) \left[\frac{\rho_{\text{cr}}(1-Y)(1+y)\sigma_T}{m_H}\right] [\{\Omega_m(1+z_r)^3 + \Omega_\Lambda\}^{1/2} - 1] \\ &= (0.00435)h_{70} [\{0.2794h_{70}^{-2}(1+z_r)^3 + 0.7206\}^{1/2} - 1], \end{aligned} \quad (2)$$

where we write $(1-Y)(1+y) = (1-3Y/4)$ and use the updated WMAP-5 parameters, $\Omega_b h^2 = 0.02265 \pm 0.00059$ and $\Omega_m h^2 = 0.1369 \pm 0.0037$. To this formula we add the extra scattering ($\tau_e \approx 0.0020$) from He III at $z \leq 3$. With this He III contribution, equation (2) yields $\tau_e = 0.040, 0.045$, and 0.050 for $z_r = 6.0, 6.5$, and 7.0 , respectively.

For large redshifts, $\Omega_m(1+z)^3 \gg \Omega_\Lambda$, and the integral simplifies to

$$\tau_e(z_r) \approx \left(\frac{c}{H_0}\right) \left(\frac{2\Omega_b}{3\Omega_m^{1/2}}\right) \left[\frac{\rho_{\text{cr}}(1-3Y/4)\sigma_T}{m_H}\right] (1+z_r)^{3/2} \approx (0.0522) \left[\frac{(1+z_r)}{8}\right]^{3/2}. \quad (3)$$

Here, we have scaled to a reionization epoch $z_r \approx 7$. From the approximate expression in equation (3), we see that $\tau_e \propto (\rho_{\text{cr}} \Omega_b \Omega_m^{-1/2} H_0^{-1})$. Thus, τ_e is nearly independent of the Hubble constant, since $\rho_{\text{cr}} \propto h^2$ while the combined parameters, $\Omega_b h^2$ and $\Omega_m h^2$, are inferred from D/H, CMB, and large-scale galaxy motions. The scaling with h therefore cancels to lowest order. A slight dependence remains from the small Ω_Λ term in equation (2).

If we invert the approximate equation (3), we can estimate the redshift of primary (Gunn-Peterson) reionization, $(1 + z_{\text{GP}}) \approx (7.77)[\tau_e(z_{\text{GP}})/0.05]^{2/3}$, scaled to the value, $\tau_e = 0.05$, expected for full ionization back to $z_{\text{GP}} \approx 7$. As discussed in § 2.2, this is approximately the WMAP-5 value of optical depth, $\tau_e = 0.084 \pm 0.016$, reduced by $\Delta\tau_e \approx 0.03$. This additional scattering, $\Delta\tau_e$, may arise from high- z star formation, X-ray preionization, and residual electrons left after incomplete recombination. The latter electrons are computed to have fractional ionization $x_e \approx (0.5 - 3.0) \times 10^{-3}$ between $z = 10$ –700 (Seager et al. 2000). Inaccuracies in computing their contribution therefore add systematic uncertainty to the CMB-derived value of τ_e . Partial ionization may also arise from the first stars (Venkatesan, Tumlinson, & Shull 2003, hereafter VTS03) and from penetrating X-rays produced by early black holes (VGS01; Ricotti & Ostriker 2004, 2005). For complete sudden reionization, Komatsu et al. (2008) estimated $z_r \approx 10.8 \pm 1.4$ at 68% C.L., by combining WMAP-5 data with other distance measures (SNe, BAO). The WMAP-5 data alone (Dunkley et al. 2008) imply $\tau_e = 0.087 \pm 0.017$, with $z_r = 11.0 \pm 1.4$ (68% C.L.). Their likelihood curves allow a range $7.5 \leq z_r \leq 13.0$ at 95% C.L. They also claim that WMAP-5 data exclude $z_r = 6$ at more than 99.9% C.L.

The additional ionization sources at $z > z_{\text{GP}}$ will contribute electron scattering that may bring the WMAP and Gunn-Peterson results into agreement for the epoch of complete reionization. In our calculations, described in § 3, we make several key assumptions. First, we assume a fully ionized IGM out to $z_{\text{GP}} \approx 6$ –7, accounting for both H^+ and ionized helium. Second, we investigate the effects of IGM partial ionization at $z > z_{\text{GP}}$. Finally, in computing the contribution of residual electrons at high redshifts, we adopt the concordance parameters from the WMAP-5 data set. The CMB optical depth is formally a 5σ result, which may improve as WMAP refines its estimates of the matter density, Ω_m , and the parameters, σ_8 and n_s , that govern small-scale power. Both σ_8 and n_s have well-known degeneracies with τ_e in CMB parameter extraction (Spergel et al. 2007; Dunkley et al. 2008). The derived parameters may change in future CMB data analyses, as the constraints on τ_e continue to evolve. In addition, inaccuracies in the incomplete recombination epoch and residual ionization history, $x_e(z)$, add uncertainties to the CMB radiative transfer, the damping of ℓ -modes, and the polarization signal used to derive an overall τ_e .

2.2. Residual Electrons in the IGM

We now discuss the contribution of residual electrons in the IGM following the recombination epoch at $z \approx 1000$. Scattering from these electrons is significant and is normally accounted for in CMB transport codes such as CMBFAST (Seljak & Zaldarriaga 1996) through the post-recombination IGM ionization history, $x_e(z)$. However, a number of past papers are vague on how the ionization history is treated and on precisely which electrons contribute to total optical depth τ_e . This has led to confusion in how much residual optical depth and damping of CMB power has been subtracted from the CMB signal. It is important to be clear on the definition of the integrated τ_e when using it to constrain the amount of high- z ionization from first-light sources. Modern calculations of how the IGM became neutral have been done by Seager et al. (2000), although their code (RECFAST) continues to be modified to deal with subtle effects of the recombination epoch and the atomic physics of hydrogen ($ns \rightarrow 1s$ and $nd \rightarrow 1s$) two-photon transitions (Chluba & Sunyaev 2007).

To illustrate the potential effects of high- z residual electrons, we have used numbers from Figure 2 of Seager et al. (2000), the top-panel model, which assumed a cosmology with $\Omega_{\text{tot}} = 1$, $\Omega_b = 0.05$, $h = 0.5$, $Y = 0.24$, and $T_{\text{CMB}} = 2.728$ K. At low redshifts, $z \approx z_r$, just before reionization, they find a residual electron fraction $x_{e,0} \approx 10^{-3.3}$. We fitted their curve for $\log x_e$ out to $z \approx 500$ to the formula:

$$x_e(z) = x_{e,0} 10^{0.001(1+z)} \approx (5 \times 10^{-4}) \exp[\alpha(1+z)] , \quad (4)$$

where $\alpha \approx 2.303 \times 10^{-3}$. More recent recombination calculations (W. Y. Wong & D. Scott, private communication) using WMAP parameters ($\Omega_b = 0.04$, $h = 0.73$, $\Omega_m = 0.24$, $\Omega_\Lambda = 0.76$) and $Y = 0.244$ find somewhat lower values, $x_{e,0} \approx 10^{-3.67}$ with $\alpha \approx 2.12 \times 10^{-3}$. The lower $x_{e,0}$ to the faster recombination rates arises from their higher assumed baryon density, $\Omega_b h^2 = 0.0213$, compared to $\Omega_b h^2 = 0.0125$ in Seager et al. (2000).

To compute the electron-scattering of the CMB from these “frozen-out” electrons, we use the same integrated optical depth formula (equation 1), in the high- z limit, where $(d\ell/dz) = (1+z)^{-1}[c/H(z)] \approx (c/H_0)\Omega_m^{-1/2}(1+z)^{-5/2}$. We integrate over the residual-electron history, from $z_r \approx 7$ back to a final redshift $z_f \gg z_r$, to find

$$\begin{aligned} (\Delta\tau_e)_{\text{res}} &= \left(\frac{c}{H_0} \right) \left[\frac{\rho_{\text{cr}}(1-Y)\sigma_T\Omega_b}{\Omega_m^{1/2}m_H} \right] \int_{z_r}^{z_f} (1+z)^{1/2} x_e(z) dz \\ &= (3.18 \times 10^{-3}) x_{e,o} \int_{(1+z_r)}^{(1+z_f)} u^{1/2} \exp(\alpha u) du . \end{aligned} \quad (5)$$

A rough estimate to the residual scattering comes from setting $\alpha = 0$ and adopting a constant

ionized fraction $x_e(z)$,

$$(\Delta\tau_e)_{\text{res}} \approx (2.12 \times 10^{-3}) \langle x_e \rangle [(1+z_f)^{3/2} - (1+z_r)^{3/2}] . \quad (6)$$

This estimate gives $\tau_e = 0.039$ for $z_r = 6$, $z_f = 700$, and $\langle x_e \rangle \approx 10^{-3}$. More precise values of τ_e can be derived from the exact integral (eq. 5) by expanding the exponential as a sum and adopting the limit $z_f \gg z_r$,

$$(\Delta\tau_e)_{\text{res}} = (0.0179) \left[\frac{(1+z_f)}{501} \right]^{3/2} \sum_{n=0}^{\infty} \frac{[\alpha(1+z_f)]^n}{(n+3/2) n!} . \quad (7)$$

For $z > 500$, the approximate formula (eq. 4) underestimates x_e , but one can integrate the appropriate curves (Seager et al. 2000) using piecewise-continuous linear fits. Table 1 lists the fitting parameters, $x_{e,0}$ and α , for various redshift ranges, together with the extra contribution, $\Delta\tau_e$. These calculations give a total optical depth in residual electrons $\Delta\tau_e \approx 0.06$ back to $z = 700$. These electrons have maximum influence on angular scales with harmonic $\ell_{\text{max}} \approx 2z^{1/2} \approx 20\text{--}50$ (Zaldarriaga 1997). At higher redshifts, x_e rises to $10^{-2.1}$ at $z = 800$ and to $10^{-1.1}$ at $z = 1000$, where the CMB source function will affect the “free-streaming” assumption used in CMBFAST (Seljak & Zaldarriaga 1996).

3. IMPLICATIONS FOR REIONIZATION MODELS

The WMAP-5 measurements (Hinshaw et al. 2008; Komatsu et al. 2008) of fluctuations in temperature (T) and polarization (E) have been interpreted to estimate *total* electron-scattering optical depth of $\tau_e \approx 0.084 \pm 0.016$. The central value comes from computing the likelihood function for the six-parameter fit to WMAP-5 data (TT, TE, EE) marginalized with BAO and SNe distance meaasures. Because of the challenges in translating a single parameter (τ_e) into a reionization history, $x_e(z)$, it is important to recognize the sizable error bars on τ_e . At 68% C.L. (Figure 1 of Komatsu et al. 2008; Figure 6 of Dunkley et al. 2008), when marginalized against other parameters such as “tilt” (n_s), the optical depth ranges from $\tau_e = 0.06 - 0.11$. The lower value is only slightly above the optical depth, $\tau_e = 0.05$, for a fully ionized IGM back to redshift $z_{\text{GP}} \approx 7$. The higher value, $\tau_e = 0.11$, clearly requires additional ionizing sources at $z > z_{\text{GP}}$.

In § 2.1, we showed that $\sim 50\%$ of this τ_e can be accounted for by a fully ionized IGM at $z \leq z_{\text{GP}}$. Observations of Ly α (Gunn-Peterson) absorption toward 19 quasars between $5.7 < z < 6.4$ (Fan et al. 2006) are consistent with a reionization epoch $z_r \approx z_{\text{GP}} = 6.1 \pm 0.15$ (Gnedin & Fan 2006). According to equation (2), this produces $\tau_e = 0.041 \pm 0.003$, where our

error propagation includes relative uncertainties in z_r (2.5%), $\Omega_m h^2$ (8.4%), and $\Omega_b h^2$ (4.0%). Detections of Ly α emitting galaxies at $z \approx 6.6$ (Hu et al. 2002; Kodaira et al. 2003; Hu & Cowie 2006) suggest that the epoch of full reionization might be as high as $z_r \approx 7$. This reionization epoch corresponds to $\tau_e \approx 0.05$ and is consistent with the small neutral fraction to which Gunn-Peterson test is sensitive, particularly when one accounts for density bias in the observed high- z ionization zones around quasars (Wyithe, Bolton, & Haehnelt 2008). Residual post-recombination electrons produce a substantial optical depth from $z \approx 10$ back to $z \approx 700$, which uniformly damps all angular scales. However, their effect on the TE and EE power is considerably less on large angular scales ($\ell \leq 10$). Thus, we can identify a significant portion of the WMAP-5 observed optical depth through known sources of ionization. The “visible ionized universe” out to $z_{\text{GP}} = 6\text{--}7$ accounts for $\tau_e = 0.04\text{--}0.05$, while high- z partial ionization could contribute additional $\Delta\tau_e \approx 0.01\text{--}0.03$. For this study, we investigate the requirements to produce an additional optical depth, $\Delta\tau_e = 0.03 \pm 0.02$, from star formation and early black hole accretion at $z > z_{\text{GP}}$.

Our calculations represent an important change in the derivation of z_r from τ_e , and suggests that the amount and efficiency of high- z star formation need to be suppressed. This suggestion is ironic, since WMAP-1 data initially found a high $\tau_e = 0.17 \pm 0.04$ (Spergel et al. 2003) implying a surprisingly large redshift for early reionization, ranging from $11 < z_r < 30$ at 95% C.L. (Kogut et al. 2003). These results precipitated many investigations of star formation at $z = 10\text{--}30$, some of which invoked anomalous mass functions, very massive stars (VMS, with $M > 140 M_\odot$), and an increased ionizing efficiency from zero-metallicity stars (VTS03; Wyithe & Loeb 2003; Cen 2003; Ciardi, Ferrara, & White 2003; Sokasian et al. 2003, 2004). Tumlinson, Venkatesan, & Shull (TVS04) disputed the hypothesis that the first stars had to be VMS. They showed that an IMF dominated by $10\text{--}100 M_\odot$ stars can produce the same ionizing photon budget as VMS, generate CMB optical depths of $0.09\text{--}0.14$, and still be consistent with nucleosynthetic evidence from extremely metal-poor halo stars (Umeda & Nomoto 2003; Tumlinson 2006; Venkatesan 2006).

Although the IGM recombination history, $x_e(z)$, is included in calculations of CMBFAST and in CMB parameter estimation, the best-fit values of τ_e from WMAP-5 and earlier CMB experiments have been attributed exclusively to the contribution from the first stars and/or black holes at $z \leq 20$. The contributions from post-recombination electrons ($20 < z < 1100$) have not always been subtracted from the data. This post-recombination contribution was relatively small in some earlier models of reionization (Zaldarriaga 1997; Tegmark & Silk 1995) that explored optical depths of $\tau_e = 0.5\text{--}1.0$ and suggested reionization epochs up to $z_r \sim 100$. However, with current data indicating late reionization, it becomes particularly important to consider contributions to τ_e at $z > z_{\text{GP}}$, prior to the first identified sources of light. The latest WMAP-5 results (Hinshaw et al. 2008) find a lower τ_e , but they also suggest more

small-scale power available for reionizing sources, owing to higher normalization parameters, $\sigma_8 \approx 0.817 \pm 0.026$ and $\Omega_m h^2 \approx 0.1369 \pm 0.0037$. This change marks a significant increase ($\Delta\sigma_8 = +0.056$) over WMAP-3 data. Between WMAP-1 and WMAP-3, the decrease in σ_8 was offset by a reduction in spectrum tilt. However, this index did not change significantly in the recent data, going from $n_s = 0.958 \pm 0.016$ (WMAP-3) to $n_s = 0.960^{+0.014}_{-0.013}$ (WMAP-5). Alvarez et al. (2006) argued, from the lower values of τ_e and σ_8 , that both WMAP-3 and WMAP-1 data require similar (high) stellar ionizing efficiencies. Haiman & Bryan (2006) use the lower τ_e to suggest that massive star formation was suppressed in minihalos. Our results on a lower $\Delta\tau_e$ make these requirements even more stringent, as we now quantify.

In the next two sub-sections, we consider two scenarios for producing partial IGM ionization at $z > z_{\text{GP}}$. The first considers ionizing UV photons from the first massive stars, which will create small “bubbles” of fully ionized gas inside ionization fronts. The second scenario examines extended partial ionization produced by X-rays from accreting black holes.

3.1. Ionization by Hot Stars

Semi-analytic and numerical models of reionization (Ricotti, Gnedin, & Shull 2002a,b; VTS03, Haiman & Holder 2003) show that the efficiency of ionizing photon injection into the IGM can be parameterized by the production rate of ionizing (UV) photons from massive stars. In our approximate models, we compute the hydrogen ionization fraction as $x_e(z) = \epsilon_{\text{UV}} f_b(z) / c_L(z)$, where $\epsilon_{\text{UV}} = N_\gamma f_* f_{\text{esc}}$ and $f_b(z)$ is the fraction of baryons in collapsed halos. To account for the nonlinearity of recombinations, we define $c_L \equiv \langle n_{\text{HII}}^2 \rangle / \langle n_{\text{HII}} \rangle^2$, the space-averaged clumping factor of ionized hydrogen. We assume that c_L is the same for H II and He III and that $N_\gamma f_* f_{\text{esc}}$ is constant with redshift. As discussed by Gnedin & Ostriker (1997), particularly in their § 3.1, clumping of the photoionized gas sharpens the reionization transition, with a recombination time much less than the local Hubble time at $z \approx 6$ –8. However, the integrated optical depth through this epoch is not greatly affected by clumping.

The main effects of clumping arise when we translate the production rate of ionizing photons into the ionization history, $x_e(z)$. When the local density of photoionized hydrogen is close to ionization equilibrium, $\langle n_{\text{HI}} \Gamma_{\text{HI}} \rangle \approx \langle \alpha_H^{(A)}(T) n_e n_{\text{HII}} \rangle$, and the quadratic dependence of recombination rates reduces the local ionization fraction by a factor c_L^{-1} . When the medium is out of equilibrium, either ionizing or recombining, this approximation, $x_e(z) = \epsilon_{\text{UV}} f_b(z) / c_L(z)$, is less accurate. To assess the validity of our approximation, we have run a set of reionization models, integrating differential equations for the propagation of ionization fronts (VTS03) to derive $x_e(z)$. When we apply our approximation with $c_L = 10$, it closely approximates the integrated hydrogen ionization history with a clumping factor of $c_L = 40$. These two curves

are virtually indistinguishable for nearly all the redshifts approaching reionization. Thus, an artificial boost by a factor of 4 in the clumping factor would correct for any deviations in our approximation from the true ionization history. Our approximation is not dramatically different in shape from the true ionization history, at least from our semi-analytic calculation, and requires at most a constant multiplicative correction in the clumping factor. We are currently pursuing numerical experiments to understand the relationship between clumping and reionization, using adaptive mesh refinement simulations (Hallman et al. 2007) and exploring different weighting schemes for clumping on the sub-grids.

The free parameters in this model are encapsulated in the “triple product”, $f_* N_\gamma f_{\text{esc}}$, where f_* represents the star-formation efficiency (the fraction of a halo’s baryons that go into stars), N_γ is the number of ionizing photons produced per baryon of star formation, and f_{esc} is the fraction of these ionizing photons that escape from the halo into the IGM. We can now use our calculations to constrain the amount of high- z star formation through the product of these three parameters. We solve for the ionization history, using our previous formalism (VTS03) in which the baryon collapse history, $f_b(z)$, is computed through the Press-Schechter formalism with the cosmological parameters from WMAP-5. The propagation of ionization fronts is followed through the production rate of ionizing photons minus recombinations.

Each of these three parameters has some dependence on the halo mass and environment (Haiman & Bryan 2006; Ricotti & Shull 2000). Since we have already parameterized the intrahalo recombinations through f_{esc} , we account for the loss of ionizing photons on IGM scales through c_L in two forms: (1) a power-law form with slope $\beta = -2$ from the semi-analytic work of Haiman & Bryan (2006); and (2) the numerical simulations of Kohler, Gnedin & Hamilton (2007), using their case C (overdensity $\delta \sim 1$ for the large-scale IGM) for C_R , the recombination clumping factor corresponding to our definition of c_L . In the latter case, the clumping factor is almost constant ($c_L \approx 6$) until the very end of reionization. Together, these two different cases provide bounds on the range of possible values, although they are quite similar over the epoch $z \approx 6$ –8 that dominates the scattering. In our calculations, we use the Haiman & Bryan (2006) formulation of $C_L(z)$.

With these assumptions, we can use equation (5) and the allowed additional optical depth, $\Delta\tau_e \leq 0.03$, to constrain the ionizing efficiency of the first stars. In Figure 1, we plot curves of efficiency factor, ϵ_{UV} , as a function of the resulting $\Delta\tau_e$. The two panels illustrate the changes in required efficiency produced by the WMAP-5 increase in “small-scale power” compared to WMAP-3 parameters. These differences arise primarily from the amplitude of fluctuations, σ_8 , which increased from $\sigma_8 = 0.761^{+0.049}_{-0.048}$ (WMAP-3) to $\sigma_8 = 0.817 \pm 0.026$ (WMAP-5). In each panel, we show two curves, corresponding to star formation in Ly α -cooled halos, with virial temperature $T_{\text{vir}} \approx 10^4$ K, and in H $_2$ -cooled minihalos ($T_{\text{vir}} \approx 10^3$ K). For these calculations, we

adopt the clumping factors from Haiman & Bryan (2006), a star-formation efficiency $f_* = 0.1$, and a range of escape fractions $f_{\text{esc}} = 0.1\text{--}0.4$. The two curves (red and blue) illustrate cases designated as Population II (metal-enriched) and Population III (zero-metal) stars. Both models adopt Salpeter initial mass functions (IMF), for which we find: (1) $N_\gamma = 60,000$ for a metal-free IMF ($10\text{--}140 M_\odot$) that agrees with both CMB and nucleosynthetic data (TVS04); and (2) $N_\gamma = 4000$ for a present-day IMF ($1\text{--}100 M_\odot$). Note that $N_\gamma = 34,000$ is consistent with $\tau_e \approx 0.084 \pm 0.016$ (WMAP-5) if photons arise from zero-metal stars (Tumlinson 2006). Values of N_γ were derived (TVS04) from the lifetime-integrated ionizing photon production from various stellar populations and IMFs and used as inputs in reionization models.

Figure 1 shows how the required additional optical depth, $\Delta\tau_e = 0.03 \pm 0.02$, translates into the efficiency required of massive stars forming in high- z halos. These plots are meant to be used as indicators of the types of star-forming halos and the stellar populations that generate ionizing photons, per baryon that passes through stars. The two panels also illustrate the sensitivity of the efficiencies to cosmological parameters (WMAP-3 vs. WMAP-5), primarily the amplitude of fluctuations, σ_8 , which sets the small-scale power of halos at a given epoch. The interpretation of Figure 1 comes from the intersection of the two rising curves (red for massive halos, blue for mini-halos) with the two green bands, which mark the range of expected efficiencies of Pop II and Pop III stars.

One can draw several general conclusions from Figure 1. First, the higher amplitude of small-scale power (larger σ_8) in the WMAP-5 results (right panel) shifts both red and blue curves to the right. Lower efficiencies of ionizing-photon production are required to produce a given additional optical depth, $\Delta\tau_e$. Second, considering just the WMAP-5 parameters (right panel), we see that “massive halos”, defined as those with $T_{\text{vir}} \approx 10^4$ K, can produce optical depths ranging from $\Delta\tau_e = 0.005\text{--}0.018$, for a range of Pop III efficiencies $\epsilon_{\text{UV}} = 600\text{--}2000$. If one invokes more plentiful mini-halos ($T_{\text{vir}} \approx 10^3$ K), reionization by Pop II stars can produce a similar $\Delta\tau_e = 0.004\text{--}0.016$. These results suggest that partial reionization at $z > z_{\text{GP}}$ could be achieved by minihalos ($T_{\text{vir}} \approx 10^3$ K), with a mixture of Pop III and Pop II stars, or a transition from one to the other, for which the rising blue curve gives $\Delta\tau_e \approx 0.02\text{--}0.06$ for $f_{\text{esc}} = 0.1\text{--}0.4$. For these minihalos, Pop II stars produce $\tau \lesssim 0.02$, but $\tau \approx 0.02\text{--}0.06$ can be achieved either by metal-poor stellar populations in halos with unusually high f_* or f_{esc} , or by metal-free massive stars in halos with very low star formation rates and/or escape fraction of ionizing radiation.

Another robust conclusion from Figure 1 is that mini-haloes ($T_{\text{vir}} = 10^3$ K) with Pop III stars can easily account for the *entire* additional optical depth ($\Delta\tau_e \approx 0.03$) needed to explain the WMAP-5 data. Even in cases where reionization begins with Pop III stars (efficiencies $\sim 10^3$) and then transitions to Pop II (efficiencies $\sim 10^2$), the optical depths are significant.

This is an important astrophysical issue, since the duration of the epoch dominated by metal-free massive first stars is still uncertain (TVS04). These results mark a significant departure from similar curves for a WMAP-3 cosmology (left panel), owing to the increased small-scale power in a WMAP-5 cosmology relative to WMAP-3. Although the scalar spectral index n_s did not change appreciably from year 3 to year 5 of WMAP, both the matter density, Ω_m , and the normalization, σ_8 , rose by several percent, an appreciable effect for power available for low-mass halos. Thus, reionization occurs slightly earlier in a WMAP-5 cosmology ($\Delta z_r \approx 1-2$) in our models, lowering the required efficiencies by a factor of about 4.

Our predictions can be compared to those of Haiman & Bryan (2006), who used WMAP-3 data to constrain the efficiency factor, ϵ_{UV} , relative to a fiducial value $\epsilon_{\text{mini}} = 200$ for minihalos. They argued that the efficiency for the production of ionizing photons must have been reduced by an order of magnitude, in order to avoid overproducing the optical depth. However, their constraints were based on the WMAP-3 value, $\tau_e \approx 0.09$, whereas half that scattering is accounted for from the fully ionized IGM at $z < z_{\text{GP}}$. In our formalism (Figure 1b), the efficiency constraints are less severe, and Pop III minihalos can easily produce $\Delta\tau_e \approx 0.06$ with the expected efficiencies, $\epsilon_{\text{UV}} \approx 10^3$. Much larger efficiencies, close to those of metal-free stellar populations, and large values of f_* and f_{esc} are required for larger halos to produce $\Delta\tau_e \approx 0.02$. It makes some difference what form is assumed for the clumping factor, c_L , in constraining the ionizing efficiency of the first stars. The level of shifts in the (red and blue) efficiency curves is comparable to the shifts between WMAP-3 and WMAP-5.

3.2. Ionization by Accreting Black Holes

The CMB optical depth also constrains the level of X-ray preionization from high-redshift black holes. Ricotti et al. (2005) were able to produce large optical depths, up to $\tau_e \approx 0.17$, using accreting high- z black holes with substantial soft X-ray fluxes. Their three simulations (labeled M-PIS, M-SN1, M-SN2) produced hydrogen preionization fractions $x_e = 0.1 - 0.6$ between $z = 15$ and $z = 10$, with large co-moving rates of star formation, $(0.001 - 0.1)M_\odot \text{ Mpc}^{-3} \text{ yr}^{-1}$, and baryon fractions, $\omega_{\text{BH}} \approx 10^{-6} - 10^{-5}$ accreted onto black holes. Any significant contribution to τ_e from X-ray preionization requires $x_e \geq 0.1$. Therefore, the lower value of τ_e from WMAP-5 reduces the allowed X-ray preionization and black-hole accretion rates significantly compared to these models. Ricotti et al. (2005) find that the IGM at $z > z_{\text{GP}}$ was highly ionized ($x_e \gg 0.01$). In this limit, there were few X-ray secondary electrons, and most of the X-ray energy went into heating the ionized medium. By contrast, the WMAP-5 optical depth suggests that the IGM was much less ionized at $z > z_{\text{GP}}$.

Relating the effects of X-ray ionization from early black holes to a $\Delta\tau_e$ and a related X-ray

production efficiency factor is less straightforward compared to the star-formation case, for the following reasons. First, unlike ionization by UV photons, X-ray ionization is non-equilibrium in nature, and the timescales for X-ray photoionization at any epoch prior to $z = 6$ typically exceeds the Hubble time at those epochs (VGS01). Therefore, it is more difficult to establish a one-to-one correspondence between X-ray production at an epoch and the average efficiency of halos. In addition, X-ray ionization (whether from stars or black holes), at least initially when $x_e < 0.1$, will be dominated by secondary ionizations from X-ray-ionized helium electrons (VGS01) rather than from direct photoionization. This may constrain the physical conditions in the IGM (e.g., the level of He ionization) rather than those in the parent halo, when we attempt to translate a $\Delta\tau_e$ into an X-ray ionization efficiency. Thus, it may be difficult to make precise inferences about the black hole density and accretion history from τ_e .

We can define an X-ray ionization rate and efficiency parameter, analogous to the previous case for massive star formation. We define $x_e(z) = \epsilon_X f_b(z)$, with no clumping factor, where $\epsilon_X = N_X f_{\text{BH}} f_{\text{esc}}$ and $f_b(z)$ is the fraction of baryons in collapsed halos. Here, f_{BH} is the average fraction of baryons in black holes in halos at $z \gtrsim 7$ and N_X is the number of X-ray ionizations of the IGM produced by X-rays and secondary ionizations, per baryon accreted onto such black holes. As we now describe, f_{BH} may approach 10^{-4} , and standard accretion estimates give $N_X \approx 10^6$ photons/baryon, so that $\epsilon_X \approx 100$.

Ricotti & Ostriker (2004) and Ricotti et al. (2005) define a parameter $\omega_{\text{BH}} = 10^{-7}$ to 10^{-6} , equal to the fraction of baryons that go into *seed* black holes. Current observations (e.g., Häring & Rix 2004) suggest that the BH-to-bulge mass fraction in modern galaxies is $M_{\text{BH}}/M_{\text{bulge}} \approx 1.4 \times 10^{-3}$. Thus, if the bulge-to-halo mass ratio is 0.065, $f_{\text{BH}} \approx 10^{-4}$, after BHs have grown from the initial fraction through accretion, thereby producing X-rays ionization at high- z . To estimate N_X , we assume Eddington-limited accretion at 10% efficiency and adopt a mean photon energy ~ 1 keV:

$$N_X \approx \left[\frac{0.1 m_p c^2}{(1.6 \times 10^{-9} \text{ erg}) E_{\text{keV}}} \right] (12) \approx (10^6 \text{ photons/baryon}) E_{\text{keV}}^{-1}. \quad (8)$$

Here, we assume that each X-ray photon produces ~ 12 hydrogen ionizations, primarily through secondary ionizations from X-ray photoelectrons (Shull & van Steenberg 1985; VGS01). In the partially ionized IGM, the free electrons come from H^+ , He^+ , and trace He^{+2} . We assume that the clumping factor (c_L) and escape fraction (f_{esc}) are roughly unity for X-rays, given their high penetrating power relative to UV photons. Figure 2 shows the allowed additional optical depth, analogous to the constraints of Figure 1, for X-ray efficiency in both Ly α -cooled halos and minihalos. Evidently, X-rays from black holes located in high-redshift minihalos can produce $\Delta\tau_e \approx 0.02$, with a substantial ionizing efficiency, $\epsilon_X \approx 100$, that rivals that of Pop II star formation.

In summary, we have shown that the revised (WMAP-5) values of CMB optical depth, $\tau_e = 0.084 \pm 0.016$, lead to a more constrained picture of early reionization of the IGM. Approximately half of the observed τ_e comes from a fully ionized IGM back to $z_{\text{GP}} \approx 6-7$. The additional $\Delta\tau_e$ at $z > z_{\text{GP}}$ probably arises from the first massive stars and from accretion onto early black holes. Some of the observed τ_e may come from scattering from residual electrons left from recombination; inaccuracies in computing this ionization history add systematic uncertainty to the CMB inferred signal. We have assumed extra scattering, $\Delta\tau_e = 0.03 \pm 0.02$ at $z > z_{\text{GP}}$ and used this to constrain the efficiencies for production and escape of ionizing photons, either by ultraviolet photons from the first massive stars (Fig. 1) or by X-rays from accretion onto early black holes (Fig. 2).

In both cases, the picture is of a partially ionized IGM at redshifts $z = 6 - 20$. For X-ray pre-ionization by early black holes, equation (6) can be used to provide an estimate of the effects of partial reionization. Between redshifts $z_2 \approx 20$ and $z_1 \approx 6$, an IGM with ionized fraction $x_{e,0} = 0.1$ (Ricotti et al. 2005) would produce $(\Delta\tau_e) = (0.018)(x_{e,0}/0.1)$, which is a significant contribution to the observed $\tau_e = 0.084 \pm 0.016$. Ricotti et al. (2005) suggested a large $x_e \approx 0.1 - 0.6$ and pushed their black-hole space densities and accretion rates to large values in order to reach the WMAP-1 estimates of $\tau_e = 0.17$. Because such large values of τ_e are no longer required, the black hole densities and IGM ionization fractions are likely to be considerably less.

All these constraints depend heavily on uncertain parameterizations of the efficiency of star formation and ionizing photon production. The most sensitive of these parameters is σ_8 , although the details of the clumping factor are comparably important. With more precise measurements of CMB optical depth from future missions, there is hope that more stringent constraints on high- z star formation and black-hole accretion will be possible. These data include additional years of WMAP observations, as well as the *Planck* mission.

Acknowledgements

We are grateful to David Spergel, Licia Verde, Rachel Bean, and Nick Gnedin for useful discussions regarding the interpretation of WMAP data and numerical simulations. We thank Douglas Scott and Wan Yan Wong for providing their calculations of recombination history. This research at the University of Colorado was supported by astrophysical theory grants from NASA (NNX07-AG77G) and NSF (AST07-07474).

Table 1. Ionization Fractions and Residual Optical Depth

Redshift Range	$x_{e,0}$ ^a	α ^a	$\Delta\tau_e$ ^b
$7 < z < 500$	5.00×10^{-4}	2.303×10^{-3}	0.0256
$500 < z < 600$	2.94×10^{-4}	3.224×10^{-3}	0.0135
$600 < z < 700$	1.28×10^{-4}	4.606×10^{-3}	0.021

^aParameters for $x_e(z) = x_{e,0} \exp[-\alpha(1+z)]$ (see text)

^bResidual integrated optical depth computed over given redshift range (see eq. 5)

REFERENCES

- Alvarez, M., Shapiro, P. R., Ahn, K., & Iliev, I. 2006, *ApJ*, 644, L101
- Becker, R., et al. 2001, *AJ*, 122, 2850
- Begelman, M. C., Volonteri, M., & Rees, M. J. 2006, *MNRAS*, 370, 289
- Cen, R. 2003, *ApJ*, 591, L5
- Cen, R., & Ostriker, J. P. 1999, *ApJ*, 519, L109
- Chluba, J., & Sunyaev, R. A. 2007, *A&A*, 480, 629
- Ciardi, B., Ferrara, A., White, S. D. M. 2003, *MNRAS*, 344, L7
- Dunkley, J., et al. 2008, *ApJS*, submitted (arXiv:0803.0586)
- Fan, X., et al. 2002, *AJ*, 123, 1247
- Fan, X., et al. 2006, *AJ*, 132, 117
- Gnedin, N. Y. 2000, *ApJ*, 535, 530
- Gnedin, N. Y. 2004, *ApJ*, 610, 9
- Gnedin, N. Y., & Fan, X. 2006, *ApJ*, 648, 1
- Gnedin, N. Y., & Ostriker, J. P. 1997, *ApJ*, 486, 581
- Haiman, Z., & Holder, G. P. 2003, *ApJ*, 595, 1
- Haiman, Z., & Bryan, G. L. 2006, *ApJ*, 650, 7
- Hallman, E. J., O’Shea, B. W., Burns, J. O., Norman, M. L., Harkness, R., & Wagner, R. 2007, *ApJ*, 671, 27
- Häring, N., & Rix, H.-W. 2004, *ApJ*, 604, L89
- Heger, A., & Woosley, S. E. 2002, *ApJ*, 567, 532
- Hinshaw, G., et al. 2008, *ApJS*, submitted (arXiv:0803.0732)
- Hu, E., et al. 2002, *ApJ*, 568, L75
- Hu, E., & Cowie 2006, *Nature*, 440, 1145
- Hui, L., & Haiman, Z. 2003, *ApJ*, 596, 9
- Kodaira, K., et al. 2003, *PASJ*, 55, L17
- Kogut, A., et al. 2003, *ApJS*, 148, 161
- Kohler, K., Gnedin, N. Y., & Hamilton, A. J. S. 2007, *ApJ*, 657, 15
- Komatsu, E., et al. 2008, *ApJS*, submitted (arXiv:0803.0547)
- Kriss, G. A., et al. 2001, *Science*, 293, 1112
- Olive, K. A., & Skillman, E. D. 2001, *New Astronomy*, 3, 119

- Page, L., et al. 2007, *ApJS*, 170, 335
- Peimbert, M., Luridiana, V., & Peimbert, A. 2007, *ApJ*, 666, 636
- Ricotti, M., & Shull, J. M. 2000, *ApJ*, 542, 548
- Ricotti, M., Gnedin, N. Y., & Shull, J. M. 2002a, *ApJ*, 575, 33
- Ricotti, M., Gnedin, N. Y., & Shull, J. M. 2002b, *ApJ*, 575, 49
- Ricotti, M., & Ostriker, J. P. 2004, *MNRAS*, 350, 539
- Ricotti, M., Ostriker, J. P., & Gnedin, N. Y. 2005, *MNRAS*, 357, 207
- Seager, S., Sasselov, D., & Scott, D. 2000, *ApJS*, 128, 407
- Seljak, U., & Zaldarriaga, M. 1996, *ApJ*, 469, 437
- Shull, J. M., & van Steenberg, M. E. 1985, *ApJ*, 298, 268
- Shull, J. M., Tumlinson, J., Giroux, M. L., Kriss, G. A., & Reimers, D. 2004, *ApJ*, 600, 570
- Sokasian, A., Abel, T., Hernquist, L., & Springel, V. 2003, *MNRAS*, 344, 607
- Sokasian, A., Yoshida, N., Abel, T., Hernquist, L., & Springel, V. 2004, *MNRAS*, 350, 47
- Spergel, D. N., et al. 2003, *ApJS*, 148, 175
- Spergel, D. N., et al. 2007, *ApJS*, 170, 377
- Tegmark, M., Silk, J., & Blanchard, A. 1994, *ApJ*, 420, 484
- Tegmark, M., & Silk, J. 1995, *ApJ*, 441, 458
- Tumlinson, J. 2006, *ApJ*, 641, 1
- Tumlinson, J., Venkatesan, A., & Shull, J. M. 2004, *ApJ*, 612, 602 (TVS04)
- Umeda, H., & Nomoto, K. 2003, *Nature*, 422, 871
- Venkatesan, A. 2006, *ApJ*, 641, L81
- Venkatesan, A., Giroux, M. L., & Shull, J. M. 2001, *ApJ*, 563, 1 (VGS01)
- Venkatesan, A., Tumlinson, J., & Shull, J. M. 2003, *ApJ*, 584, 621 (VTS03)
- White, M., Scott, D., & Silk, J. 1994, *ARA&A*, 32, 319
- Wyithe, J. S. B., & Loeb, A. 2003, *ApJ*, 586, 693
- Wyithe, J. S. B., Bolton, J. S., & Haehnelt, M. G. 2008, *MNRAS*, 383, 691
- Zaldarriaga, M. 1997. *Phys. Rev. D*, 55, 1822
- Zheng, W., et al. 2004, *ApJ*, 605, 631

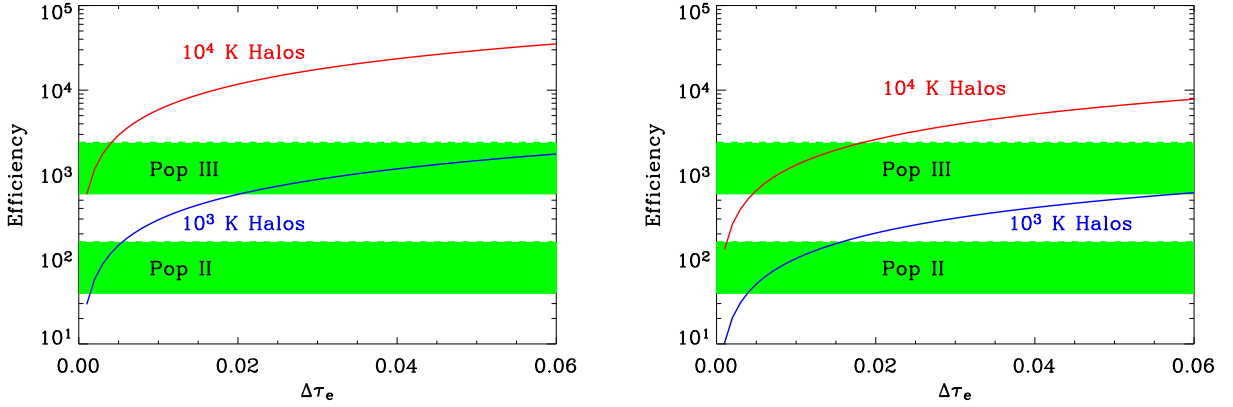


Fig. 1.— Locus of efficiency factors, $\epsilon_{\text{UV}} = N_{\gamma} f_{*} f_{\text{esc}}$, for production and escape of photoionizing radiation vs. additional optical depth, $\Delta\tau_e$, from hot stars at $z > z_{\text{GP}}$. Models assume cosmological parameters from WMAP-3 (left panel) and WMAP-5 (right panel). WMAP-5 found more small-scale power (higher σ_8) for mini-halo ionization, hence lower required efficiencies. Efficiency, $\epsilon_{\text{UV}} = f_{*} N_{\gamma} f_{\text{esc}}$, is defined (§ 3.1) for star formation in Ly α -cooled massive halos (red curve, $T_{\text{vir}} \geq 10^4$ K) and in H $_2$ -cooled minihalos (blue curve, $T_{\text{vir}} \geq 10^3$ K). Green horizontal bands correspond to expected efficiencies for a Salpeter stellar IMF: $\epsilon_{\text{UV}} \approx 600$ –2000 for metal-free Pop III (10–140 M_{\odot}) and $\epsilon_{\text{UV}} \approx 40$ –150 for metal-enriched Pop II (1–100 M_{\odot}). We adopt star-formation efficiency $f_{*} = 0.1$ and photon escape fraction f_{esc} ranging from 0.1–0.4 (see § 3.1 for details). The intersection of the rising red curve (right panel) with the upper green band shows that Pop III halos ($T_{\text{vir}} \approx 10^4$ K) can produce $\Delta\tau_e \approx 0.01$ –0.02. The intersection of the rising blue curve with the two bands shows that mini-halos ($T_{\text{vir}} \approx 10^3$ K) can produce $\Delta\tau_e = 0.01$ –0.02 (Pop II) and $\Delta\tau_e$ up to 0.06 (Pop III/Pop II).

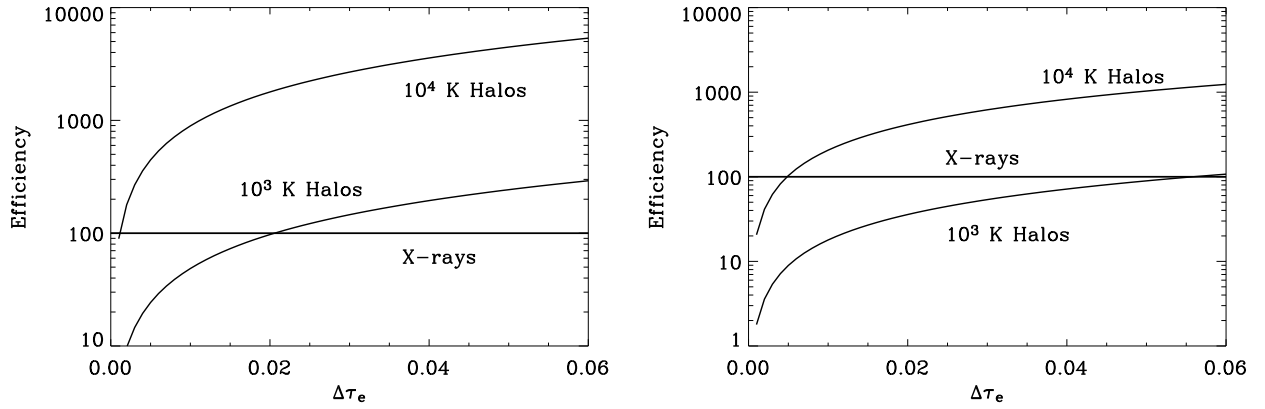


Fig. 2.— X-ray production efficiency, $\epsilon_X = N_X f_{\text{BH}} f_{\text{esc}}$, required to produce additional optical depth, $\Delta\tau_e$, at $z > z_{\text{GP}}$. We assume that $f_{\text{esc}} = 1$ for X-rays. This efficiency is the product of the baryon fraction in black holes times the total ionizations produced per accreted baryon. Curves are for WMAP-3 parameters (left) and WMAP-5 (right). The required efficiencies are lower for WMAP-5 parameters, with their additional small-scale power. Two curves are shown, for halos with virial temperatures of 10^3 K and 10^4 K. Horizontal curves show a fiducial value, $\epsilon_X \approx 100$, equivalent to $f_{\text{BH}} \approx 10^{-4}$, $N_X \approx 10^6$ (see § 3.2), and $f_{\text{esc}} = 1$.